# A Low-Distortion Oblique Map Projection of the World's Landmasses

Krisztián Kerkovits
*Eötvös Loránd University*
kerkovits@map.elte.hu

*This study presents the development of a world map projection intended to minimize distortion of all continents. I begin by reviewing a very similar map projection developed by Canters (2002), and address its shortcomings by carefully fine-tuning the initial constraints and the method of optimization, while retaining the most useful ideas of this earlier map. Most notably, the method described in this paper puts a great emphasis on the outline of the map, so that its aesthetics make it more suitable for atlases; the method also exclusively uses reproducible, deterministic methods. Finally, I compare the resulting world map to the original one of Canters in terms of map distortions and practical usefulness. The method presented here should work without changes if a low-distortion map of any other global-scale area is needed.*

**KEYWORDS:** world map; map projections; numerical optimization; polynomial approximation; Airy–Kavrayskiy criterion

## BACKGROUND

"A MAP PROJECTION IS THE MAPPING OF A CURVED surface, especially a sphere or ellipsoid, into a plane" (Lapaine 2017). It is evident that map projections distort our view of the Earth, but their application is inevitable. On one hand, when compared to a physical or virtual globe, flat maps are easier to store (or are easier displayed on a flat screen) and provide an easier overview of relations covering more than a hemisphere. On the other hand, the distortions of map projections are generally a disadvantage that we need to eliminate as much as possible.

We should note that although the reduction of map distortion is a traditional approach in cartography, it is not the only meaningful workflow. Some maps are intentionally distorted to visualize a particular dataset, such as showing the areas of political units in proportion to their populations, or by spacing locations not by their physical distance, but based on the travel time between points. The reader may find further information on the theory and mathematics behind such intentionally distorted map projections (known as cartograms) in Gastner, Seguy, and More (2018). In this paper, however, the aim will be to minimize distortion with respect to the geographic reality.

The theory of Meshcheryakov (1968) states that for each area there exists an "ideal projection" that has the lowest amount of distortion possible for that area. The exact solution is still an open problem for general areas, but there are plenty of methods to approximate this map projection by polynomials or similar series. The ideal projection is strongly coupled to the region it was optimized for: each subset of the sphere will have a different ideal projection.

Although this paper deals with world maps, I will not minimize distortion for the full globe; apart from a few exceptions, a map's primary theme is usually confined to either the continents or the world ocean. As I have already previously investigated a low-distortion map of the world ocean (Kerkovits 2022), the domain of the optimization in this paper will instead be the landmasses of the earth. As the result will be a world map, the ~20 km difference between a sphere and the actual shape of the earth will not be considered; this difference diminishes to insignificance at the smaller map scales usually used for world maps.

Most world maps are plotted in a normal aspect. However, the distribution of the continents is highly asymmetrical

about the equator, leading to an imbalance of distortion. Landmasses near the poles, such as Antarctica, are often distorted into unrecognizable shapes. This means that in the optimal map, the aspect of the projection (Lapaine and Frančula 2016) should be rotated, so that continents are far from the new "poles," which are called *metapoles* or *pseudopoles*. This is just a spatial rotation of the sphere, and it allows us to move our area of interest into the most advantageous parts of the projection. The most general aspect of a map projection (i.e., neither angle of rotation is a multiple of 90°) is called a *plagal aspect* by Wray (1974). Applying of plagal aspect mappings makes the most sense if Antarctica is important in our map (this is the weak point of most normal aspect world maps), and the optimization in this study will consider Antarctica as important as any other continent.

## AN EARLIER, SIMILAR WORK

Canters (2002, 209–212) has already proposed a world map in plagal aspect with similar design principles to the one I will present here. Canters used random pairs of points and compared their mapped distances to their original ones. He adjusted the parameters of the map projection using the downhill simplex method until the average difference in distance could not be reduced further. However, his resulting map has several shortcomings:

- The methodology of Canters is reproducible only in a statistical sense. Furthermore, the consideration of such finite elements inevitably suffers from the "edge effect" (Albinus 1981; Laskowski 1997; Kerkovits 2019), so the peripheral parts of continents (i.e., areas near the coasts) have less weight during the optimization. The method I will present uses a deterministic method to determine the best fitting parameters, which also resolves the edge effect.

- Canters did not find the optimal aspect parameters for his oblique maps. I experimented with the downhill simplex method using different initial values and found that the arrangement of Canters is only a local minimum with respect to the distortion. In most cases, the downhill simplex method converged to a neighborhood of another minimum described later in this paper. That one has a lower distortion value, and so it is a more likely candidate to be the global minimum.

- The outline of a map projection is irrelevant for regional maps, where the cartographer may crop the map by a frame of arbitrary shape. However, it is a crucial aesthetic point for world maps, where the map frame is exactly the border of the map projection. Apparently, Canters did not consider this; therefore, his map has a very unusual shape (Figure 1). It bends concave near the metaequator (pseudoequator) and has sharp concave corners at the metapoles. My proposed projection puts a great emphasis on the outline of the final map.

Thus, one may consider this paper as an attempt to improve the methods and the map of Canters, while trying to keep the advantages of the original design.

## DESIGN CONSIDERATIONS

The map presented in this paper has been designed to show continents with low distortions. However, these distortions must be measured on an infinitesimal scale: distortion measurements of finite shapes are all based on random samples, and thus are not reproducible in a strict sense. Deterministic methods are preferred. Furthermore, random samples are not distributed uniformly; due to the edge effect they are a bit sparser near the boundaries of the area. In this study, coastal regions are regarded as equally important compared to inland parts. Therefore, the Airy–Kavrayskiy criterion described later in Equation 14 was chosen to be the distortion value of the optimization.

Ideal map projections, despite their name, are not necessarily the "best" mappings. They have unusual properties that can hinder their aesthetic value. Most prominently, as the distribution of continents is asymmetrical on the earth, it is obvious that their ideal map is also asymmetrical. However, the map frame should be symmetrical
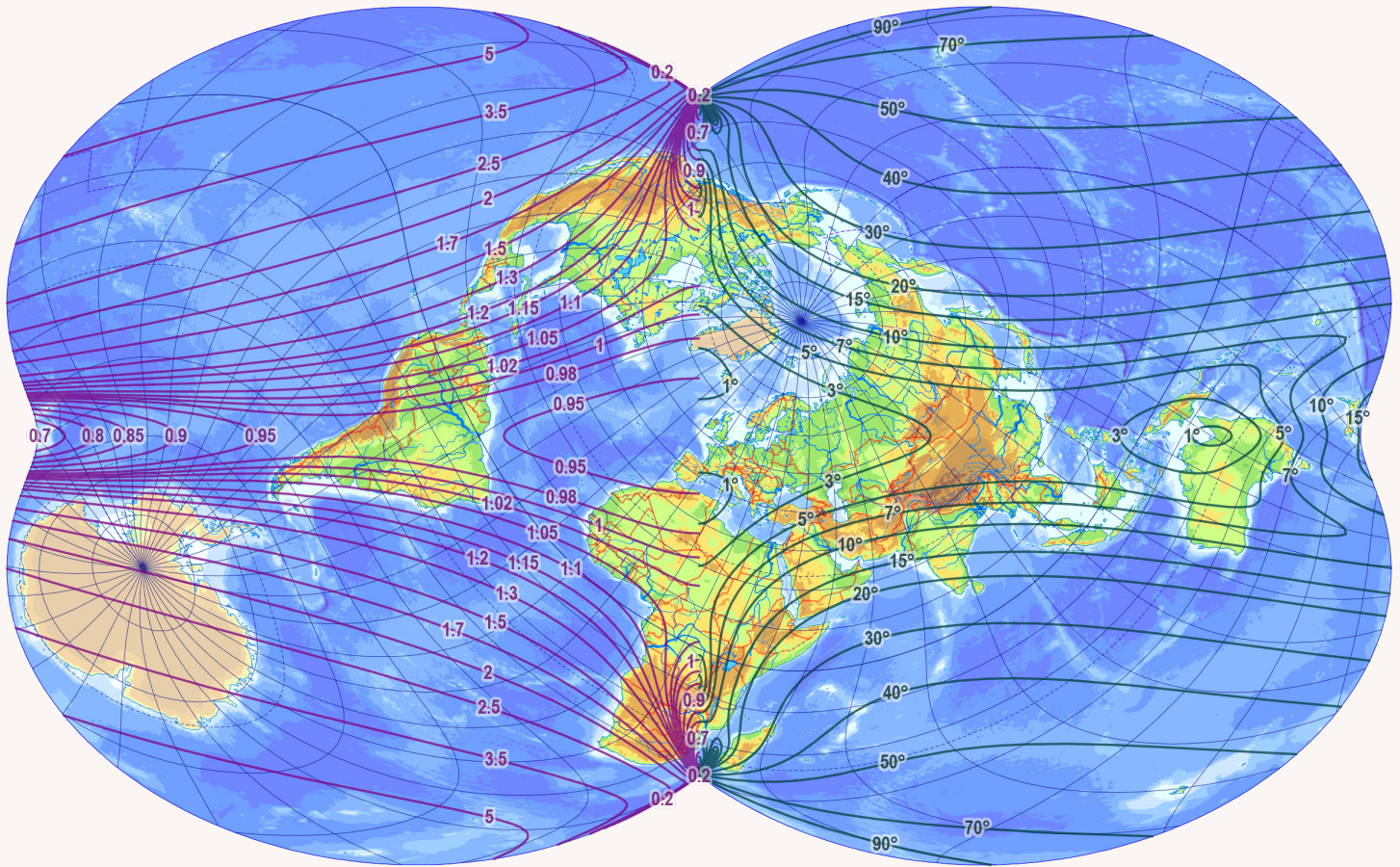
**Figure 1.** The plagal map projection of Canters (2002, 213) Purple lines: areal scale, green lines: maximal angular deviation.

to resemble the symmetries of the underlying sphere. Therefore, the map projection developed here will be symmetrical about both the metaequator and the prime metameridian. This ensures the symmetry of the map frame and the distortion distribution. Nevertheless, the map graticule will be asymmetrical due to the plagal aspect.

It is well known that flat-polar maps can have, in general, lower distortions than pointed-polar ones (Snyder 1985, 124). However, flat-polar oblique world maps are not encountered in serious publications, and oblique world maps of established authors (e.g., Bartholomew, Briesemeister) are all pointed-polar. A possible reason is that while map readers are accustomed to seeing the true pole represented by a pole line, the same is not accepted in the case of an arbitrary metapole. It's worth noting that there *are* some

oblique flat-polar maps, by authors such as Winkel and Wagner, but these have their metapoles placed outside the map frame. Consequently, the map projection developed here will be pointed-polar.

We must also observe that in oblique world maps, such as previous examples like the Atlantis or the Bertin projections, the metapole is never cusped (like in the sinusoidal projection), but the map frame is smooth. Assuming that this decision comes from aesthetic consideration, this study will prescribe that the map frame must be smooth at the metapoles. Furthermore, metameridians (except the prime metameridian) will also pass through the metapole without a cusp, so that graticule lines will continue smoothly (an example of such a map is that of Mollweide).

## FORMULAE OF THE MAP PROJECTION

In the mathematical development of the new map, we will assume that the earth is a sphere of unit radius. Following the usual convention, $\varphi$ will stand for

latitude and longitude will be denoted as $\lambda$. Unless explicitly marked by a degree symbol, all angles are in radians. The image of the map projection is on the plane

parametrized by a usual Cartesian coordinate system. Planar coordinates are denoted by $x$ and $y$.

The formulae of the map projection must be developed with due care. The exact formulation influences the result of the optimization significantly (Canters 2002). We must allow the map projection to take any possible shape permitted by the prior constraints. Assuming that the optimal projection is smooth (analytical), a polynomial can approximate it to arbitrary precision. On the other hand, simple polynomials permit flat-polar projections. A map projection symmetrical about its mid-meridian is pointed-polar if

$$x|_{\varphi=\pm\frac{\pi}{2}} = 0 \quad \text{and} \quad \frac{\partial y}{\partial \lambda}\bigg|_{\varphi=\pm\frac{\pi}{2}} = 0 \tag{1}$$

Bimeridians will cross the pole without a cusp if they are perpendicular to the vertical axis:

$$\lim_{\varphi\to\pm\frac{\pi}{2}}\frac{\partial x}{\partial \varphi} = \pm\infty \tag{2}$$

The simplest function that satisfies the constraints of $x$ is achieved by transforming the equation of a circle:

$$x = P_x(\varphi,\lambda)\sqrt{1-\left(\frac{2\varphi}{\pi}\right)^2} \tag{3}$$

where $P_x(\varphi, \lambda)$ can be any polynomial of $\varphi$ and $\lambda$.

The constraint on $y$ is less specific, as it only requests that its derivative must be zero at two points. It may either be achieved by a quadratic function or a cosine function. Testing both ideas, it turned out that the latter one behaved better (allowed for more flexibility during optimization) when being multiplied by the polynomial, so $\partial y/\partial\lambda$ was chosen to be $P'_y(\varphi, \lambda)\cos\varphi$. Integrating it with respect to $\lambda$ yields

$$y = P_y(\varphi,\lambda)\cos\varphi + P_c(\varphi) \tag{4}$$

where $P_c(\varphi)$ is a constant of integration, which is a polynomial of $\varphi$, and $P_y(\varphi, \lambda)$ is the antiderivative of polynomial $P'_y(\varphi, \lambda)$. Namely, $P_y(\varphi, \lambda)$ can be almost any polynomial, but it must not contain terms constant in $\lambda$.

Symmetry about the mid-meridian and the equator can be achieved by constraining the parity of functions $x$ and $y$. In our case, $P_x$ must be an even function of $\varphi$ and an odd function of $\lambda$, $P_y$ must be an odd function $\varphi$ of and an

even function of $\lambda$, and $P_c$ must be an odd function of $\varphi$. Putting this together:

$$\begin{aligned}x = (A_{01}\lambda + A_{03}\lambda^3 + A_{21}\varphi^2\lambda + A_{05}\lambda^5 \\ + A_{23}\varphi^2\lambda^3 + A_{41}\varphi^4\lambda + \cdots)\sqrt{1-\left(\frac{2\varphi}{\pi}\right)^2}\end{aligned} \tag{5}$$

$$\begin{aligned}y = (B_{12}\varphi\lambda^2 + B_{32}\varphi^3\lambda^2 + B_{14}\varphi\lambda^4 + \cdots)\cos\varphi \\ + B_{10}\varphi + B_{30}\varphi^3 + B_{50}\varphi^5 + \cdots\end{aligned} \tag{6}$$

The polynomials were truncated at the fifth degree. A major problem was that even with fifth-degree polynomials, I found seemingly completely different sets of coefficients as local minima with different starting values, but there was absolutely no visual difference in the resulting maps, and their estimated distortion value was different by less than 0.0001%. This experience suggests that a better approximation might be meaningless.

Additionally, I examined seventh-degree polynomials. However, the computation time was more than 10 hours on a modern desktop computer, compared to the more reasonable 20–30 minutes needed for optimizing the fifth-degree polynomial. This made it cumbersome to check different starting values, although the downhill simplex method seemed to be very sensitive to them: it reported local minima very far from each other, none of which could be responsibly reported as a global minimum. Nevertheless, the resulting maps were close in appearance to the result of the fifth-degree polynomial, so that there appeared to be no practical benefit from using higher-degree polynomials.

This resulting map projection can then be applied in the plagal aspect to further minimize distortion. Namely, the metapole is rotated to a point at $\varphi_0$, $\lambda_0$, and the prime metameridian has azimuth $\lambda'_p$. In this case, the metalatitude $\varphi'$ and metalongitude $\lambda'$ becomes (Snyder 1987):

$$\varphi' = \arcsin[\sin\varphi_0\sin\varphi + \cos\varphi_0\cos\varphi\cos(\lambda-\lambda_0)] \tag{7}$$

$$\lambda' = -\lambda'_p + \arctan\frac{\sin(\lambda-\lambda_0)}{-\cos\varphi_0\tan\varphi + \sin\varphi_0\cos(\lambda-\lambda_0)} \tag{8}$$

but it should be noted that the *arctan* function should actually be implemented as *atan2* in many conventional programming languages.

When applying Equations 5 and 6, the metacoordinates obtained in Equations 7 and 8 should be substituted for $\varphi$ and $\lambda$.

# OPTIMIZATION OF COEFFICIENTS

Coefficients $A_{ij}$, $B_{ij}$ and parameters $\varphi_o$, $\lambda_o$, $\lambda'_p$ of the aspect were optimized against the Airy–Kavrayskiy criterion (denoted as $E$) calculated as (Györffy 2018):

$$h = \sqrt{\left(\frac{\partial x}{\partial \varphi}\right)^2 + \left(\frac{\partial y}{\partial \varphi}\right)^2} \qquad (9)$$

$$k = \frac{1}{\cos\varphi}\sqrt{\left(\frac{\partial x}{\partial \lambda}\right)^2 + \left(\frac{\partial y}{\partial \lambda}\right)^2} \qquad (10)$$

$$\cot\vartheta = \frac{\frac{\partial x}{\partial \lambda}\frac{\partial x}{\partial \varphi} + \frac{\partial y}{\partial \lambda}\frac{\partial y}{\partial \varphi}}{\frac{\partial x}{\partial \lambda}\frac{\partial y}{\partial \varphi} - \frac{\partial y}{\partial \lambda}\frac{\partial x}{\partial \varphi}} \qquad (11)$$

$$a = \frac{\sqrt{h^2 + k^2 + 2hk\sin\vartheta} + \sqrt{h^2 + k^2 - 2hk\sin\vartheta}}{2} \qquad (12)$$

$$b = \frac{\sqrt{h^2 + k^2 + 2hk\sin\vartheta} - \sqrt{h^2 + k^2 - 2hk\sin\vartheta}}{2} \qquad (13)$$

$$E = \sqrt{\frac{1}{S}\iint_S \frac{\ln^2(ab) + \ln^2\frac{a}{b}}{2}\,dS} = \sqrt{\frac{1}{S}\iint_S \ln^2 a + \ln^2 b\,dS} \qquad (14)$$

where $S$ is the surface of continents.

The surface integral in Equation 14 should be calculated over irregular spherical polygons. It was, in fact, evaluated numerically using the two-point Gaussian quadrature generalized for spherical polygons (Kerkovits 2020). Optimal parameters were found by a more robust variant of the downhill simplex method as designed by Kaczmarczyk (1999).

Simultaneous optimization of the aspect parameters and coefficients made the method unstable, converging into various local minima. Therefore, in the first step, only the aspect parameters were optimized, trying a few starting values. Most runs resulted in $\varphi_o \approx 37.8711°$, $\lambda_o \approx 168.0160°$, $\lambda'_p \approx -140.8168°$, which is quite far from what Canters (2002) reported: $\varphi_o \approx 30°$, $\lambda_o \approx -140°$, $\lambda'_p \approx 150°$ using the notation conventions of this study. Furthermore, a few starting values led the downhill simplex to other local minima: notably, one of the local minima was pretty close to the values Canters reported and showed only slightly bigger distortion values (see exact values in the next section) after optimizing the coefficients: $\varphi_o \approx 19.1366°$, $\lambda_o \approx -118.2273°$, $\lambda'_p \approx 140.1385°$. Some selected starting values that I tried can be checked in Table 1. Minima were considered identical if they resulted in the same map upside down.

It seems that Canters only found a local minimum for the aspect parameters. Although Canters excluded Antarctica from the optimization, the optimal map projection has circa 3.27% less distortion if we use the aspect parameters developed here instead of Canters's one, even if Antarctica is excluded from the calculation. The result of this correction is that Antarctica will be moved from the bottom right corner to the bottom left one, and the antimeridian cut will go through the Drake Passage instead of passing by the Kerguelen Islands. Cartographic effects of this change are discussed at the end of the paper.

In the second step, the aspect parameters were fixed and only coefficients were optimized. Allowing the aspect parameters to change, distortions would have been decreased

| Starting value | | | Terminated at |
| --- | --- | --- | --- |
| $\varphi_o$ | $\lambda_o$ | $\lambda'_p$ | |
| 90° | 0° | 0° | Global minimum |
| 90° | 0° | 90° | Other local minimum |
| 90° | 0° | 180° | Canters's minimum |
| 90° | 0° | -90° | Canters's minimum |
| 45° | 0° | 0° | Global minimum |
| 45° | 90° | -90° | Global minimum |
| 45° | -90° | 90° | Global minimum |
| -45° | 0° | 0° | Other local minimum |
| 0° | 0° | 0° | Global minimum |
| 0° | 90° | 0° | Global minimum |
| 0° | 180° | 0° | Canters's minimum |
| 0° | -90° | 0° | Other local minimum |
| 0° | 0° | 90° | Canters's minimum |
| 0° | 0° | 180° | Global minimum |

**Table 1.** Influence of starting values on the result of aspect parameter optimization.

further, but the map frame would have cut into the middle of South America, which is clearly unacceptable for a map projection that is themed around continents. As an aesthetic consideration, angles of the aspect parameters were rounded to the nearest 5° so that the graticule lines of the map would symmetrically "snap" to the map frame. The starting projection was the Apian II ($A_{ij} = B_{ij} = 0$ but $A_{01} = B_{10} = 1$), but in order to avoid reporting local minima, the downhill simplex method was restarted near the result of the last run and the result was accepted only if two successive runs reported the same minimum.

## THE RESULTING MAP PROJECTION

AS MENTIONED PREVIOUSLY, TWO SETS OF ASPECT parameters were tried. The first, $\varphi_o = 20°$, $\lambda_o = -120°$, $\lambda'_p = 140°$ (close to Canters's original suggestion) resulted in $E \approx 0.186371$, while the new parameters of $\varphi_o = 40°$, $\lambda_o = 170°$, $\lambda'_p = -140°$ lead the optimization to $E \approx 0.178772$. Therefore, the previous set of parameters were discarded. Finally, the calculated coefficients are: $A_{01} \approx 0.843705$, $A_{03} \approx 0.009100$, $A_{21} \approx 0.028176$, $A_{05} \approx -0.001242$, $A_{23} \approx -0.001448$, $A_{41} \approx 0.063196$, $B_{10} \approx 0.953366$, $B_{30} \approx 0.033826$, $B_{12} \approx 0.015131$, $B_{50} \approx -0.006287$, $B_{32} \approx -0.025215$, $B_{14} \approx 0.008227$.

Substituting this into Equations 5–8, one gets the map displayed in Figures 2–4. The reader is advised to compare the distortion isolines to that of Canters's original map (Figure 1). It can be observed that both angular and areal distortions decreased significantly at most places. The biggest winner is, of course, Antarctica, where areal inflation decreased from 150% to only 10%, and the angular deviation was changed from 20° to 7°. Other regions gaining much better representation include South Africa (inflation: 100% → 50%; angular deviation: 40° → 25°) and Mexico (inflation: 50% → −2%; angular deviation: 25° → 12°). Weak points of the new mapping are in Australia (inflation almost unchanged; angular deviation: 3° → 12°) and Chile (inflation: 0% → 12%; angular deviation effectively the same). In general, the new projection surpasses Canters's one.
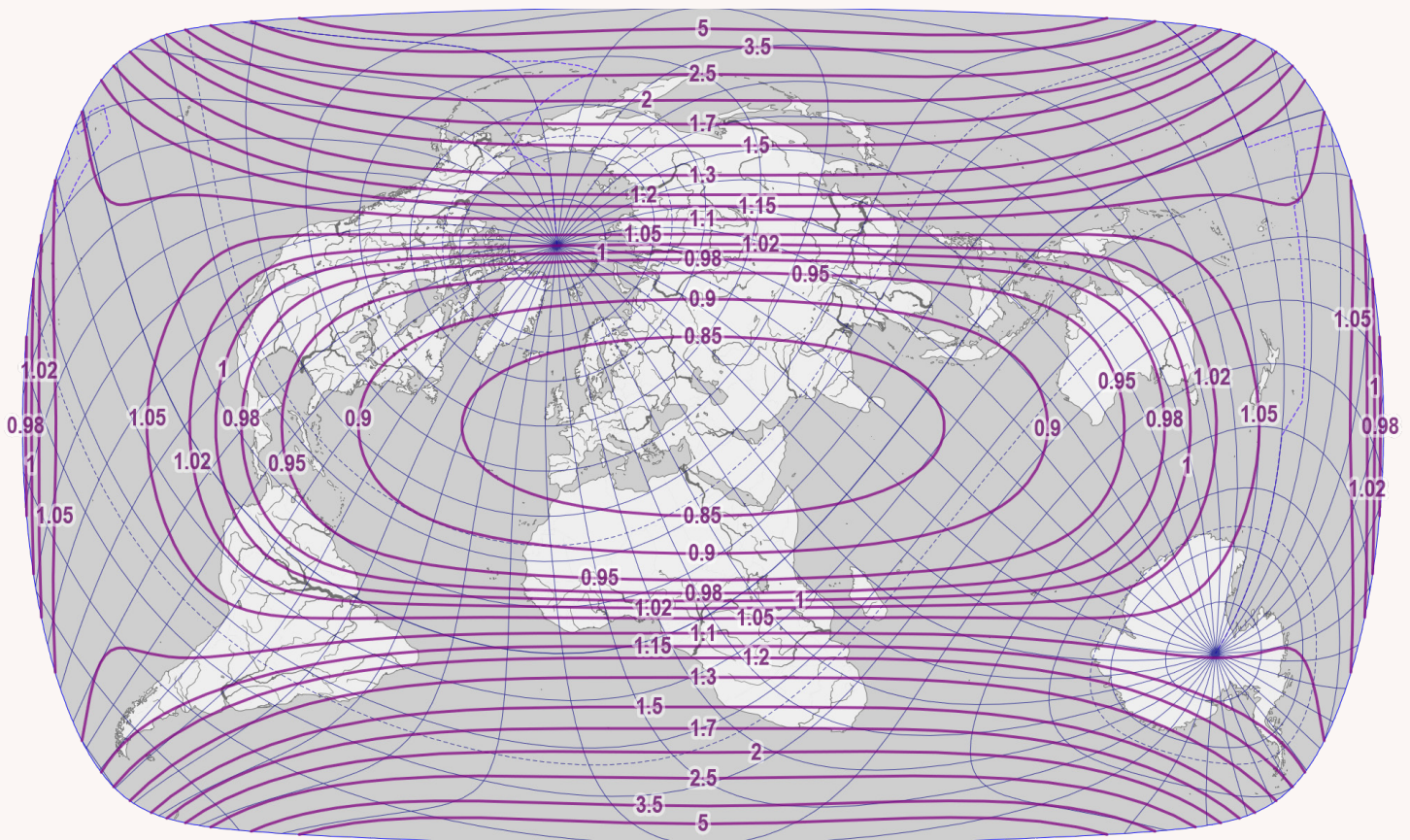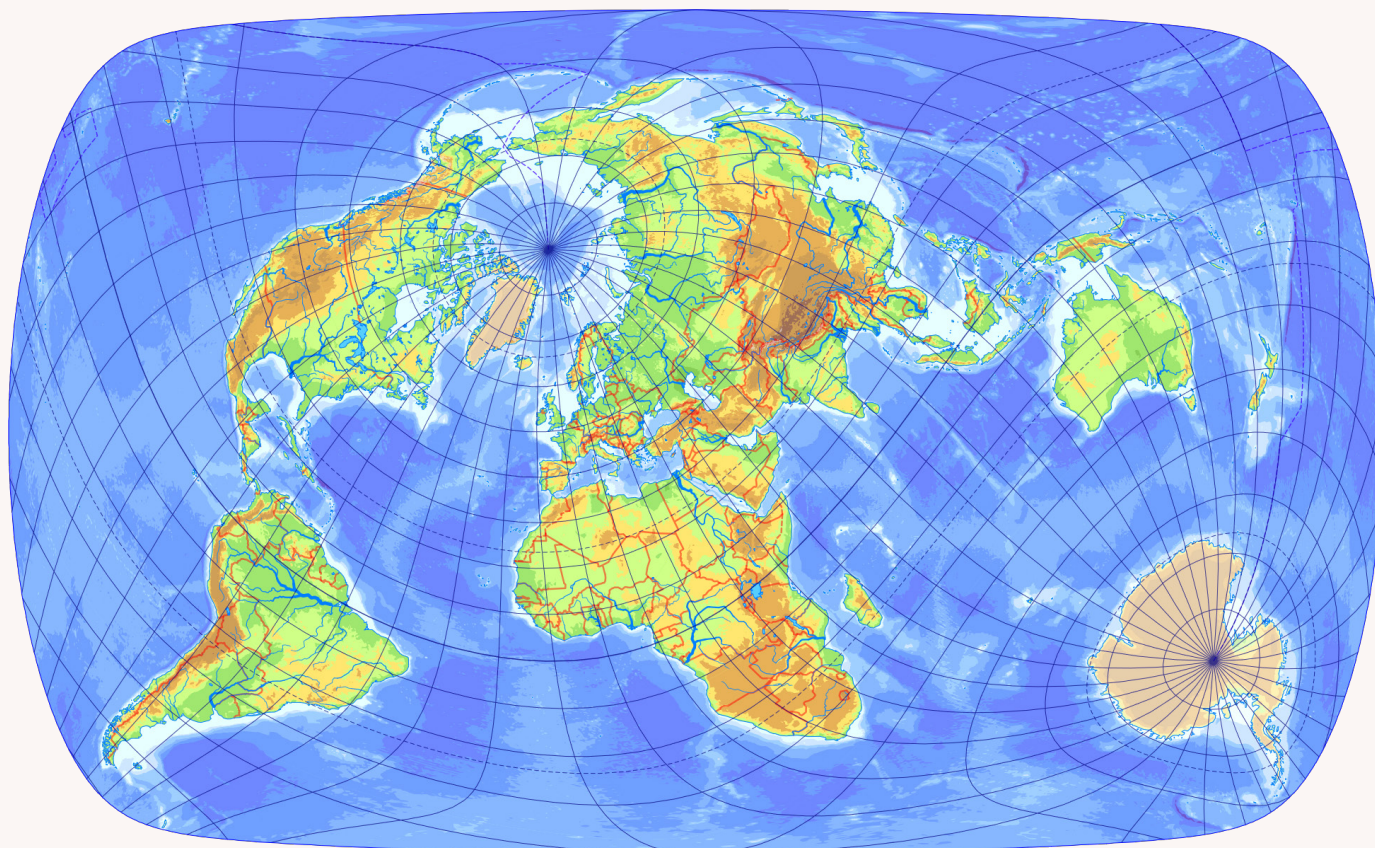


**Figure 2.** The new map projection developed in this paper (isolines of areal scale).
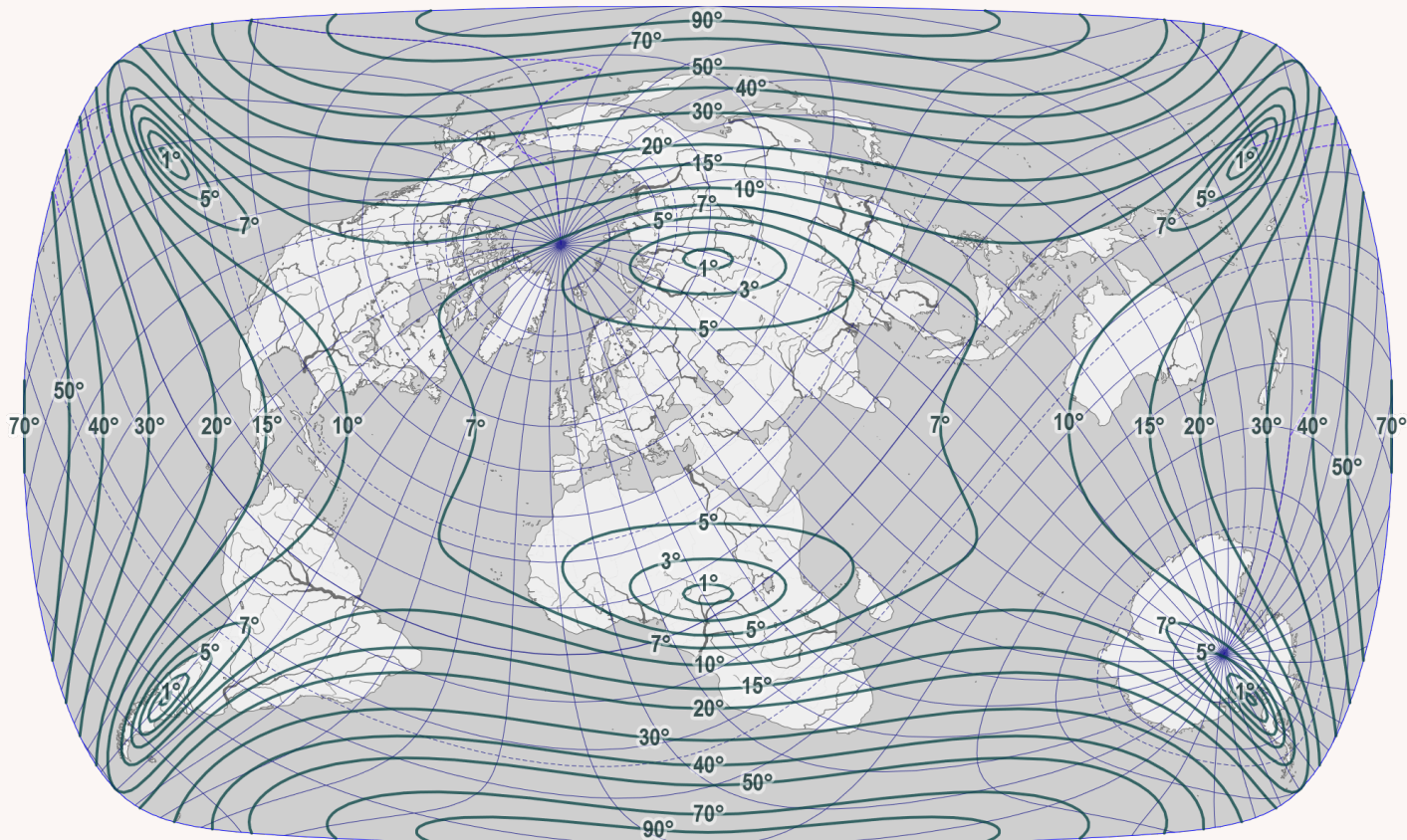
**Figure 3.** The new map projection developed in this paper (isolines of maximum angular deviation).



**Figure 4.** The new map projection developed in this paper (without isolines)

## CONCLUSIONS

COMPARING THE OVERALL TEXTURE OF THE NEW map to that of Canters, the map presented here is significantly more compact. Continents appear to be closer to each other, emphasizing their global connections. However, the different placement of the discontinuity at the antimeridian has stretched the southern tip of Africa slightly away from South America, and the connection between Antarctica and South America is lost. These disadvantages are, however, not so large: South Africa and Argentina are quite far from each in reality, and one can hardly find a map theme in which global connections between South America and Antarctica would be crucial. However, for situations where such proximities do matter, the present map can show the proximity of New Zealand to Antarctica or even to its outlying islands, which is a feature absent from Canters's map.

The amount of distortion was already quite low, but it could even be reduced further by trying to avoid local minima and carefully selecting the functions used in the development. This paper used fifth-degree polynomials for the approximation, as the computation technology has not advanced enough since Canters to allow for a better approximation.

The frame of the resulting map looks like a rounded rectangle. This might be considered as an advantage, as it fits well in a rectangular screen or a rectangular sheet of paper. However, this shape has very low resemblance to the near-spherical shape of the Earth. Nevertheless, it still fills a typical page better than Canters's apple-shaped frame, and the lack of the concave bends make it a more reasonable solution for practical cartography. Although according to my own aesthetic taste, further correction of the outline is unnecessary in this case; if one needs a more "elliptical" outline, it should be possible to combine the method presented in this paper with the outline reshaping method of Györffy (2018).

As a final thought, the present study shows that after a wise choice of design criteria, optimal map projections of the earth do not always look unnatural. The results of the optimization presented here may be used as-is in practical cartography.

## REFERENCES

Albinus, Hans-Joachim. 1981, "Anmerkungen und Kritik zur Entfernungsverzerrung." *Kartographische Nachrichten* 31 (5): 179–183.

Canters, Frank. 2002. *Small-scale map projection design.* London: CRC Press. https://doi.org/10.4324/9780203472095.

Gastner, Michael T, Vivien Seguy, and Praytush More. 2018. "Fast flow-based algorithm for creating density-equalizing map projections." *Applied Mathematics* 115 (10): 2156–2164. https://doi.org/10.1073/pnas.1712674115.

Györffy, János. 2018. "Minimum distortion pointed-polar projections for world maps by applying graticule transformation." *International Journal of Cartography* 4 (2): 224–240. https://doi.org/10.1080/23729333.2018.1455263.

Kaczmarczyk, Grzegorz. 1999. "Downhill simplex method for many dimensions." Accessed March 16, 2002. http://paula.univ.gda.pl/~dokgrk/simplex.html.

Kerkovits, Krisztián. 2019. "Comparing finite and infinitesimal map distortion measures." *International Journal of Cartography* 5 (1): 3–22. https://doi.org/10.1080/23729333.2018.1500255.

———. 2020. "Quadrature Rules to Calculate Distortions of Map Projections." *The Cartographic Journal* 57 (3): 249–260. https://doi.org/10.1080/00087041.2020.1714278.

———. 2022. "A Low-Distortion Map of the World Ocean Without Discontinuities." *Kartografija i Geoinformacije* 21 (special issue): 80–90. https://doi.org/10.32909/kg.21.si.6.

Lapaine, Miljenko. 2017. "Definicija kartografske projekcije [Map Projection Definition]." *Kartografija i Geoinformacije*. 28 (16): 136–137. English translation is available at https://kig.kartografija.hr/index.php/kig/article/view/795.

Lapaine, Miljenko, and Nedjeljko Frančula. 2016. "Map projection aspects." *International Journal of Cartography*. 2 (1): 38–58. https://doi.org/10.1080/23729333.2016.1184554.

Laskowski, Peter. 1997. "Part 1: Distortion-spectrum fundamentals a new tool for analyzing and visualizing map distortions." *Cartographica* 34 (3): 3–18. https://doi.org/10.3138/Y51X-1590-PV21-136G.

[Meshcheryakov, German A.] Мещеряков, Герман А. 1968. Теоретические основы математической картографии [Theoretical bases of mathematical cartography]. Москва: Недра.

Snyder, John P. 1985. *Computer-assisted map projection research*. Washington, DC: US Government Printing Office. https://doi.org/10.3133/b1629.

———. 1987. *Map projections: A working manual*. Washington, DC: US Government Printing Office. https://doi.org/10.3133/pp1395.

Wray, Thomas. 1974. "The Seven Aspects of a General Map Projection." *Cartographica* 11 (2): 1–72. https://doi.org/10.3138/E382-8522-4783-28K5.